2016

A library of infectious hepatitis C viruses with engineered mutations in the E2 gene reveals growth-adaptive mutations that modulate interactions with scavenger receptor class B type I

Adam Zuiani
Washington University School of Medicine

Kevin Chen
Washington University School of Medicine

Megan C. Schwarz
Icahn School of Medicine

James P. White
Washington University School of Medicine

Vincent C. Luca
Stanford University School of Medicine

See next page for additional authors

An E2 gene infectious HCV library reveals growth adaptive mutations that modulate interactions with the scavenger receptor class B type I

Adam Zuiani[1], Kevin Chen[2], Megan C. Schwarz[6], James P. White[3], Vincent C. Luca[7], Daved H. Fremont[1,2,4], David Wang[1,2], Matthew J. Evans[6], and Michael S. Diamond[1,2,3,5]

Departments of Pathology and Immunology[1], Molecular Microbiology[2], and Medicine[3], Biochemistry and Molecular Biophysics[4], and the Center for Human Immunology and Immunotherapy Programs[5], Washington University School of Medicine, St. Louis, MO. [6]Department of Microbiology, Icahn School of Medicine at Mount Sinai, New York, NY. [7]Departments of Molecular and Cellular Physiology and Structural Biology, and the Howard Hughes Medical Institute, Stanford University School of Medicine, Stanford, CA 94305, USA.

Address correspondence to:

Michael S. Diamond, M.D. Ph.D., Departments of Medicine, Molecular Microbiology, and Pathology and Immunology, Washington University School of Medicine, 660 South Euclid Ave. Box 8051, Saint Louis, MO 63110, USA. diamond@borcim.wustl.edu, (314) 362-2842

Figures: 7; Tables: 4

Running title: Adaptive HCV E2 mutations modulating SR-BI interaction

ABSTRACT

While natural hepatitis C virus (HCV) infection results in highly diverse quasispecies of related viruses over time, mutations accumulate more slowly in tissue culture, in part because of the inefficiency of replication in cells. To create a highly diverse population of HCV particles in cell culture and identify novel growth-enhancing mutations, we engineered a library of infectious HCV with all codons represented at most positions in the ectodomain of the E2 gene. We identified many putative growth adaptive mutations and selected nine highly represented E2 mutants for further study: Q412R, T416R, S449P, T563V, A579R, L619T, V626S, K632T, and L644I. We evaluated these mutants for changes in particle to infectious unit ratio, sensitivity to neutralizing antibody or CD81 large extracellular loop (CD81-LEL) inhibition, entry factor usage, and buoyant density profiles. Q412R, T416R, S449P, T563V and L619T were neutralized more efficiently by anti-E2 antibodies and T416R, T563V and L619T by CD81-LEL. Remarkably, all nine variants showed reduced dependence on scavenger receptor class B type I (SR-BI) for infection. This shift from SR-BI usage did not correlate with a change in the buoyant density profiles of the variants, suggesting an altered E2-SR-BI interaction rather than changes in the virus-associated lipoprotein-E2 interaction. Our results demonstrate that residues influencing SR-BI usage are distributed across E2 and support the development of large scale mutagenesis studies to identify viral variants with unique functional properties.

43 **IMPORTANCE**

44 Characterizing variant viruses can reveal new information about the lifecycle of
45 Hepatitis C virus (HCV) and the roles played by different viral genes. However, it is difficult to
46 recapitulate high levels of diversity in the laboratory because of limitations in the HCV culture
47 system. To overcome this limitation, we engineered a library of mutations into the E2 gene in
48 the context of an infectious clone of the virus. We used this library of viruses to identify nine
49 mutations that enhance the growth rate of HCV. These growth enhancing mutations reduced the
50 dependence on a key entry receptor, scavenger receptor class B type I (SR-BI). By generating a
51 highly diverse library of infectious HCV, we mapped regions of the E2 protein that influence a
52 key virus-host interaction and provide proof-of-principle for the generation of large-scale mutant
53 libraries for the study of pathogens with great sequence variability.
54

INTRODUCTION

Hepatitis C virus (HCV) infection causes a major global health burden, as approximately 3% of the world's population is affected (1). Up to 30% of individuals with HCV will resolve infection spontaneously, whereas the majority develop chronic infections that can cause fibrosis, cirrhosis, and hepatocellular carcinoma (2). HCV is a member of the hepacivirus genus of the *Flaviviridae* family of RNA viruses, and is a positive-sense, enveloped virus with a 9.6 kilobase genome. The genome comprises a single open reading frame encoding an approximately 3,000 amino acid polyprotein flanked by 5′- and 3′- noncoding regions. HCV primarily infects and replicates in hepatocytes, and its lifecycle is tied intimately to the lipoprotein biosynthesis pathway. HCV particles incorporate host lipoproteins forming a "lipoviroparticle" with unique properties when compared to other *Flaviviridae* members (3, 4).

HCV is divided into 7 genotypes and 67 subtypes and exists as a quasispecies within a host (5). Natural HCV isolates exhibit considerable diversity in their genomic sequences, however it is difficult to recapitulate the extent of this variability *in vitro.* Recent advances have made it possible to infect cells in culture with human-derived HCV isolates and observe genome replication, but new infectious particles still cannot be generated readily from clinical samples (6). The study of cell culture infectious HCV relies on a few, relatively slow-growing infectious clones (7–13). These clones do not acquire growth adaptive mutations rapidly during passaging despite the high error rate of the HCV polymerase, possibly because of the limited production of new infectious virions.

HCV has two envelope glycoproteins, E1 and E2. The E2 gene is a protein of particular variability and is under selection pressure from adaptive immune responses during an extended chronic infection (14, 15). In conjunction with virus-associated lipoprotein, the envelope proteins mediate attachment and entry of the virus into host cells (16). E1 and E2 form non-covalently linked trimers of disulfide-linked heterodimers on the virion surface (17, 18). Two partial crystal structures of the "core" of the E2 protein have provided some insight into E2

structural biology (19, 20). E2 core has a compact, globular structure consisting mainly of random coils and β-strands. While several structural features of E2 have well-described functions in the HCV lifecycle, the contributions of other regions of the protein are less well understood (21–24).

To study an HCV population containing an array of single amino acid variants, we created a genotype 2a JFH-1 isolate library with maximal diversity in the E2 gene. We generated a site-directed saturation mutagenesis (SDSM) library from a JFH-1-derived infectious clone, which allowed us to explore almost the entire sequence space for single-codon substitutions in E2. We used the library to identify novel E2 growth adaptive mutations. After only three passages, nine mutations in different regions of the protein were identified and confirmed to have growth kinetic advantages: Q412R, T416R, S449P, T563V, A579R, L619T, V626S, K632T, and L644I. These mutants had varying profiles with respect to neutralizing monoclonal antibody (NMAb) and CD81 large extracellular loop (CD81-LEL) sensitivity. However, all of these mutations yielded a reduced dependence on scavenger receptor class B type I (SR-BI) for entry even though they were distributed across several regions of E2. Our study provides insight into the molecular determinants of the interaction between SR-BI and E2 and acts as proof-of-principle for the use of large scale variant libraries to address questions in HCV biology.

METHODS AND MATERIALS

Cell culture. Huh7.5 cells were obtained as a gift (C. Rice, Rockefeller University) and maintained in Dulbecco's Modified Eagle Medium (DMEM, Thermo Fisher Scientific) supplemented with 10% fetal bovine serum (FBS, Equitech-Bio), MEM nonessential amino acids, and penicillin/streptomycin (Corning).

Plasmid library and virus production. The plasmid pLJ83, which encodes the JFH-1 HCV infectious clone bearing adaptive mutations outside of the E2 gene, was a generous gift (G. Luo, University of Alabama, Birmingham) (25) and used for our SDSM library. Unless noted in the text, all amino acid residues numbers refer to the JFH-1 genome (26). Three hundred and twenty complementary primer sets containing random nucleotides at all three positions of a single codon within the E2 gene were designed and ordered from Integrated DNA Technologies. All residues between amino acid positions 384 and 721 in the polyprotein were targeted, excluding cysteines (positions 429, 452, 459, 488, 496, 505, 510, 554, 566, 571, 585, 589, 601, 611, 624, 648, 656, and 681). Each primer set was used to amplify variants by polymerase chain reaction (PCR) from pLJ83 using a Phusion® high fidelity polymerase kit (New England Biolabs). The PCR products were digested with *Dpn*I (New England Biolabs) and transformed in library-grade MegaX® DH10B T1R electrocompetent cells (Thermo Fisher Scientific).

Plasmids were prepared from bacterial cultures using plasmid Maxi-prep kits (Qiagen) from sets of ten sequential codon libraries generated by SDSM. The 32 pooled plasmid libraries corresponded to the following amino acids: 384-393, 394-403, 404-413, 414-423, 424-434, 435-444, 445-455, 456-466, 467-476, 477-486, 487-498, 499-509, 511-520, 521-530, 531-540, 541-550, 551-561, 562-573, 574-583, 584-595, 596-606, 607-617, 618-628, 629-638, 639-649, 650-660, 661-670, 671-680, 682-691, 692-701, 702-711 and 712-721. The plasmids were linearized by digestion with *Nru*I (New England BioLabs), purified, and genomic RNA was synthesized using a MEGAscript T7 transcription kit (Ambion). Infectious HCV was generated after transfection of Huh7.5 cells as follows: 2 µg of *in vitro*-derived viral RNA was electroporated into

4 x 10^6 Huh7.5 cells, and virus was harvested 48, 72, 96, and 120 h later. HEPES pH 7.3 (10 mM) was added to the virus-containing supernatants for storage at 4°C prior to concentration with Amicon Ultra 100,000 kDa MWCO centrifugal filters (EMD Millipore). Concentrated virus stocks were stored at -80°C and titered using the 50% tissue culture infectious dose ($TCID_{50}$) method (27).

Amplicon sequencing of plasmid libraries. The 32 sets of pooled plasmids described above were analyzed using next generation sequencing to determine the diversity of the library. An approximately 2 kilobase fragment corresponding to the E1 and E2 genes was amplified by PCR from each of the 32 plasmid pools and submitted for Ampicon-seq library preparation and Illumina HiSeq sequencing (single end 50 basepair reads) at the Genome Technology Access Center at Washington University. Reads were aligned to the pLJ83 sequence using Bowtie2. Reads containing insertion or deletions were not considered, and the remaining reads were counted to determine codon frequency using a custom script.

Focus-forming assay. Infectious HCV was detected using a focus-forming assay (FFA) on Huh7.5 cells. Briefly, 6.4 x 10^3 Huh7.5 cells were plated in individual wells of a 96-well plate treated with of poly-L-lysine one day prior to infection. Three days later, cells were rinsed with PBS, fixed and permeabilized with cold methanol, rinsed again and incubated in blocking solution (PBS containing 1% BSA and 0.2% skim milk). Subsequently, the cells were incubated with 100 ng/mL anti-NS5A mAb (9E10, a gift of C. Rice, Rockefeller University (9)), rinsed again, and incubated with 1:2000 dilution of horseradish peroxidase conjugated goat anti-mouse IgG (Sigma). Virally-infected cell foci were visualized using TrueBlue™ peroxidase reagent (KPL) and quantified using an S5 Biospot™ Macroanalyzer (Cellular Technologies Ltd).

Selection of mutations in E2 that confer increased HCV growth. Parallel cultures of 3.8 x 10^4 Huh7.5 cells were infected with 1 x 10^4 $TCID_{50}$ of each of 32 HCV mutant pools containing engineered diversity at ten sequential positions in E2. Input viruses were removed 6 h post-infection and newly generated viruses were harvested 7 days later and used to infect

new Huh7.5 cells. This process was performed twice for a total of three passages. After the third passage, viral RNA was harvested using QIAamp® viral RNA mini kits (Qiagen) from all 32 final passage viruses, cDNAs were synthesized using the Superscript III® first strand synthesis system (Invitrogen), and DNA fragments corresponding to the E1-E2 fragment were amplified by PCR. Each PCR product was sequenced across the region of the E2 gene containing the sites of engineered mutations in the original pool. If changes to the consensus sequence were observed, the exact combinations of nucleotide substitutions at any given codon were determined using a Zero Blunt® TOPO® PCR Cloning Kit (Invitrogen) to generate individual bacterial colonies bearing unique E1-E2 sequences. Nine mutations identified from the TOPO cloning results were introduced into pLJ83 using conventional site-directed mutagenesis. Following verification of the complete genome sequence of the mutant plasmids, all nine clonal mutant viruses were generated as described above. Three of the nine selected mutations (S449P, L619T and L644I) also were introduced into a JFH-1-derived chimeric infectious clone encoding the structural genes of the genotype 1 H77 isolate (H77/JFH-1) at homologous positions in the E2 gene (28). The corresponding mutations in the H77 strain were S449P, L615T and L640I. Virus was produced exactly as described above, except an *Xba*I instead of *Nru*I restriction enzyme digestion was performed prior to *in vitro* RNA production.

Alignment of genotype 2 E2 amino acid sequences. To determine if the substitutions selected were present in circulating HCV strains, an alignment of genotype 2 E2 sequences was generated using the NIAID Virus Pathogen Database and Analysis Resource (ViPR) (http://www.viprbrc.org/) (29).

HCV growth analysis. Huh7.5 cells were infected at a multiplicity of infection (MOI) of 0.1 with parent virus or clonal growth-adapted mutants. Input viruses were removed 6 h post-infection and samples collected every 24 h for seven days. Viral yield in the supernatant was quantified by FFA. The FFA protocol increased the apparent number of infectious units of growth adapted virus in a sample slightly because of the more rapid growth and spread to new

177 cells by the mutants. We therefore performed a second growth kinetic analysis using the $TCID_{50}$
178 method of virus titration to quantify virus. Huh7.5 cells were infected at an MOI of 0.05 with each
179 of the clonal growth-adapted mutants as described above, and viral yield in supernatant was
180 collected 5 days post-infection and calculated.

181 **HCV genome quantification.** qRT-PCR was used to quantify genome copy number in
182 virus-containing supernatants. Viral RNA was harvested using QIAamp® Viral RNA Mini Kit
183 (Qiagen). All reactions were prepared using a TaqMan® RNA-to-C_T™ (Applied Biosystems),
184 with forward primer 5′-GATAAACCCACTCTATGCCCG-3′, reverse primer 5′-
185 CTATCAGGCAGTACCACAAGG-3′, and probe 5′-5′-/56-FAM/CTTTCGCAACCCAACGCTACT
186 CG-/36-TAMSp/-3′. Run conditions were 48°C for 15 min, 95°C for 10 min, and then 40 cycles of
187 95°C for 15 s an 60°C for 1 min. *In vitro* transcribed genomic transcripts were used as
188 standards.

189 **Inhibition of HCV infection by anti-E2 NMAbs and CD81 large extracellular loop.**
190 Two-hundred $TCID_{50}$ of parent or mutant viruses were pre-incubated with a dilution series of
191 anti-E2 antibody or CD81-LEL for 1 h at 37°C and then added to Huh7.5 cells. Infection was
192 quantified 72 h later by FFA, and EC_{50} values determined after performing non-linear regression
193 analysis. Anti-E2 antibodies HC84.26 (a gift of S. Foung, Stanford University) and H77.39 have
194 been described (30, 31). To generate soluble CD81-LEL, residues 114-203 of human CD81
195 were cloned into a Pet28(+)-derived vector with a thrombin cleavable C-terminal BirA
196 biotinylation site and 6xHis tag. CD81-LEL was produced by isopropyl β-D-1-
197 thiogalactopyranoside induction in BL21-DE3 *E. coli* cells and purified by oxidative refolding
198 from inclusion bodies (32). Briefly, bacterial cell pellets were resuspended in a 1:1 mixture of
199 solution buffer (50 mM Tris [pH 8.0], 25% sucrose, 10 mM dithiothreitol [DTT]), and lysis buffer
200 (50 mM Tris [pH 8.0], 1% Triton X-100, 100 mM NaCl, 10 mM DTT). The sample was lysed by
201 sonication and centrifuged, and the pellets were washed three times with wash buffer (50 mM
202 Tris [pH 8.0], 0.5% Triton X-100, 100 mM NaCl, 1 mM DTT) and once in wash buffer without

Triton X-100 to obtain purified inclusion bodies. The purified inclusion body pellets were resuspended in TE buffer (10 mM Tris [pH 8.0], 1 mM EDTA), and aliquots of the slurry were solubilized in 6 M guanidine-HCl, 10 mM Tris (pH 8.0), and 20 mM β-mercaptoethanol. Solubilized aliquots were diluted rapidly into a stirring reservoir of oxidative refolding buffer (400 mM L-Arginine, 100 mM Tris [pH 8.0], 0.5 mM oxidized glutathione, 5 mM reduced glutathione) followed by overnight incubation. The refolded CD81-LEL then was purified by size-exclusion chromatography.

Inhibition of infection by antibodies against HCV entry factors. Huh7.5 cells were treated with serially diluted anti-CD81, anti-claudin-1 (CLDN1), or anti-SR-BI antibodies for 1 h at 37°C and then infected with 200 $TCID_{50}$ of parent or mutant viruses. Infection was quantified 72 h later by FFA, and EC_{50} values were determined after non-linear regression analysis. Anti-CD81 (clone JS-81) was purchased from BD Biosciences, and anti-CLDN1 (clone 5.16v5, a gift of I. Hotzel, Genentech), and anti-SR-BI (clone mAb16-71, a gift of A. Nicosia, CEINGE Biotecnologie Avanzate, Naples, Italy) were obtained from colleagues (33, 34).

CRISPR/Cas9 mediated gene editing of SR-BI. To perform CRISPR/Cas9 mediated gene editing, we generated expression plasmids encoding the U6 promoter in front of SR-BI specific guide RNAs (35). Two rounds of overlapping PCR were performed by amplifying a guide RNA encoding plasmid (provided by George Church, Harvard University, Boston, MA, Addgene plasmid # 41819): in the first round, PCR products were generated encompassing the U6 promoter through the 5′ end of the guide RNA (consisting of the specific target sequence) with the ME-O-1122 oligonucleotide (5′-CGGGCCCCCCCTCGAGTGTACAAAAAAGCAGGCT-3′) and an SR-BI target sequence specific reverse oligonucleotide (see list below). A second PCR product was generated encompassing a region from the SR-BI target sequence through the end of the guide RNA coding sequence with a forward direction CLDN1 target sequence specific oligonucleotide (ME-O-1138; 5′-GCTTCATTCTCGCCTTCCGTTTTAGAGCTAGAAATA-3′). These products were re-amplified with only the outside oligonucleotides, ME-O-1122 and -

1123, to produce single PCR products flanked by *Xho*I and *Eco*RI sites at the 5′ and 3′ ends, respectively, that were cloned into pBlueScript. Four separate SR-BI specific gRNA plasmids were created with the following forward and reverse oligonucleotide combination: ME-O-1241/1242; 5′-CTGCTCCGCCAAAGCGCGC GTTTTAGAGCTAGAAATA-3' / 5'-GCGCGCTTTGGCGGAGCAG CGGTGTTTCGTCCTTTCC-3′, ME-O-1243/1244; 5′-GGCCCTACGTGTACAGGTG GTTTTAGAGCTAGAA ATA-3′ / 5′-CACCTGTACACGTAGGGCC CGGTGTTTCGTCCTTTCC-3′, ME-O-1245/1246; 5′-CCCTCCAAGTCCCACGGCT GTTTTAGAGCTAGAAATA-3′ / 5′-AGCCGTGGGACTTGGAGGG CGGTGTTTCGTCCTTTCC-3′, and ME-O-1247/1248; 5′-GATCCACCTCGTGGACAAG GTTTTAGAGCTAGAAATA-3′ / 5′- CTTGTCCACGAGGTGGATC CGGTGTTTCGTCCTTTCC-3′, which target nucleotides 5259-5277, 51409-51427, 53942-53960, and 57068-57086 of the SR-BI human genomic locus (relative to Genbank accession number NG_028199), respectively.

Huh7.5 cells were transiently transfected with expression plasmids encoding a human codon optimized Cas9 protein from *Streptococcus pyogenes* (provided by George Church, Harvard University, Boston, MA, Addgene plasmid # 41815) (35) and a pooled mixture of the above SR-BI guide RNA expression plasmids. Transfected cells were passaged for one to two weeks to allow the turnover of previously translated target protein. Cells were then subjected to fluorescence activated cell sorting (FACS) for loss of SR-BI following staining with the anti-SR-B1 antibody (mAb16-71) and a goat anti-human Alexa-647 antibody (Invitrogen, Carlsbad, CA). Knockout of SR-BI efficiency prior to sorting was 11-15%. Single cell clones were obtained by limiting dilution cloning in 96-well plates. Individual clones were expanded and assayed for SR-BI expression by flow cytometry with the mAb16-71 antibody, and the capacity to support HCV infection, as previously described (9). We chose Huh7.5 SR-BI^{KO} clone 16 as a representative single cell clone for further experiments.

254 **Lentiviral transduction of SR-BI^{KO} Huh7.5.** Transgene expression through lentiviral
255 transduction was used to complement SR-BI^{KO} cells. To express GFP alone, the self-
256 inactivating lentiviral provirus TRIP-GFP-linker was used (31). For SR-BI expression, the TRIP-
257 GFP-hu-SR-BI-linker provirus was used. VSV-G pseudotyped lentiviral stocks were produced in
258 293T cells, as previously described (31, 36). Supernatants were collected 2 days post
259 transfection and used to infect gene-edited Huh7.5 cells, also as previously described (31, 36).
260 Cells were expanded for at least two weeks prior to analysis.

261 **Infection of SR-BI gene-edited Huh7.5 cells**. SRBI^{KO}+GFP or SRBI^{KO}+GFP+SR-BI
262 cells (1 x 10^5) were plated in wells of a poly-L-lysine treated 96-well plate one day prior to
263 infection. Seventy-five $TCID_{50}$ of virus per well were added, and three days later the plates were
264 developed by FFA. Relative infection was calculated by determining the percent of foci present
265 in SRBI^{KO}+GFP wells compared to SRBI^{KO}+GFP+SRBI wells for each virus.

266 **Virus attachment to gene-edited Huh7.5 cells**. SR-BI^{KO}+GFP or SRBI^{KO}+GFP+SR-BI
267 cells (5 x 10^5) in suspension were incubated with 5 x 10^4 $TCID_{50}$ of virus for 3 h on ice. Cells
268 were washed 6 times with chilled media and cellular RNA was harvested using a Qiagen
269 RNeasy® Mini Kit. Viral genome copies were measured by qRT-PCR as described above.
270 Relative attachment was calculated by determining the percentage of viral RNA bound to
271 SRBI^{KO}+GFP cells compared to SRBI^{KO}+GFP+SRBI cells for each WT and mutant virus.

272 **Sucrose density gradient ultracentrifugation.** HCV was ultracentrifuged using 5-50%
273 (w/v) sucrose gradient ultracentrifugation. Sucrose solutions were prepared in TEN buffer (0.01
274 M Tris, pH 8.0; 1 mM EDTA, and 100 mM NaCl) using a Gradient Master (Biocomp). The
275 viruses were ultracentrifuged for 17 h at 4°C and 105,000 x g (Beckman SW41 Ti) and 1 ml
276 fractions were collected and titered by FFA. The number of genome copies in each fraction was
277 determined by RT-PCR as described above. Fraction densities were measured using an ABBE-
278 3L refractometer (Thermo Fisher Scientific).

Statistical analysis. Statistical analyses were performed using GraphPad Prism software. Differences in mean EC_{50} values, relative infections, titers or RNA:$TCID_{50}$ values between the mutants and parent virus were analyzed by one way-ANOVA followed by a Dunnett's test.

283 **RESULTS**

284 **Isolation of adaptive JFH-1 variants by passage of a library containing**
285 **mutagenized E2 genes.** Several growth adaptive mutations have been previously identified in
286 E2 and studying the properties of these mutants is an established method of linking structural
287 features of E2 with functions in the virus lifecycle (37–41). Past attempts to identify growth
288 adaptive mutations in the HCV genome have relied on serial passage of a clonal virus stock for
289 weeks or months until adaptive mutations arise (25, 38–50). To identify adaptive mutations
290 more expediently, we created a library of infectious HCV with a fully mutagenized E2
291 ectodomain (**Fig 1A**). Three hundred and twenty primer sets containing three random
292 nucleotides (NNN) corresponding to one codon in the ectodomain of E2 were designed. Using
293 these primers and a JFH-1 infectious clone plasmid, we performed separate SDSM reactions
294 with each primer pair yielding 320 plasmid libraries. To simplify production of infectious virus, we
295 grouped the plasmid libraries into 32 sets of 10 adjacent codons for all downstream steps. To
296 confirm that each plasmid library contained 64 engineered variants (all nucleotide combinations
297 at each codon) we performed amplicon sequencing of the 32 sets of 10 pooled single codon
298 plasmid libraries (**Fig 1B**). Under ideal conditions we expected a 10% mutation rate for a single
299 codon within the ten plasmid pool containing variability at that position; our library had an
300 average mutation rate of 6.0%. To produce infectious HCV, we transcribed RNA genomes *in*
301 *vitro* from the pooled plasmids and electroporated each of 32 RNA stocks into Huh7.5 cells. By
302 the end of this process, we had created 32 viral "pools" with each containing maximum
303 variability at ten positions in E2.

304 Following virus production, cultures of Huh7.5 cells were inoculated with 10^4 $TCID_{50}$ of
305 each of the 32 mutant pools at a MOI of 0.3. Input virus was removed 6 h after infection and
306 newly produced virus was collected 7 days later. This output virus was used to infect Huh7.5
307 cells serially twice more after which Sanger sequencing of HCV E2 RT-PCR products was
308 performed. Eight of the 32 third passage (P3) viruses had changes in the consensus sequence

of E2 within the region containing engineered variability. To determine the specific substitutions that were enriched by passaging, we generated cDNA from P3 viruses, and TOPO-cloned the E1-E2 genome fragment amplicons produced by PCR. We sequenced the E2 gene for 24 to 48 resultant bacterial colonies from each of the 8 P3 viruses with consensus sequence changes (**Table 1**).

Based on these results, nine variants that corresponded to the dominant amino acid substitution in each of the P3 viruses were selected for further study: Q412R, T416R, S449P, T563V, A579R, L619T, V626S, K632T, and L644I. Four of these residues (Q412, T416, S449 and T563) are at or very near to positions in E2 that have been reported as adaptive mutations (38–41, 45), with the remainder not having been described to affect growth. Sequencing of individual clones suggested that multiple substitutions at a given position might confer growth advantage over the parent virus with the exception of S449, which had only proline substitutions. S449P also was unique, as it eliminated a predicted N-linked glycosylation site at N448.

Clonal mutant viruses show enhanced growth kinetics. We used conventional site directed mutagenesis to introduce the nine dominant mutations into the parental infectious clone. Following verification by complete genome sequencing of the plasmids, mutant viruses were generated after electroporation of *in vitro* derived RNA into Huh7.5 cells and titered using the $TCID_{50}$ method. To validate the significance of the mutations, multi-step viral growth analyses were performed by FFA after infection of Huh7.5 cells (MOI of 0.1) with each mutant and the parental virus (**Fig 2A**). Whereas each of the mutations conferred a growth advantage compared to the parental virus, we noticed that the input virus titer (t = 0) for all of the mutant viruses appeared higher than the parent JFH-1 in this assay. Because we inoculated with equivalent input amounts based on the $TCID_{50}$ assay, we hypothesized that the difference at t = 0 of the input virus reflected the more rapid growth of the adaptive mutant strains over the course of the FFA compared to WT virus. Given this potential confounding issue, we performed

335 a second confirmatory viral growth assay. Cultures of Huh7.5 cells were infected at an MOI of
336 0.05 (as determined by $TCID_{50}$ assay) with the mutant and parent viruses, and supernatants
337 were collected five days later and titered by $TCID_{50}$ assay (**Fig 2B**). Using this second method,
338 the mutants exhibited a 5- and 10-fold growth advantage compared to the parental viruses. In
339 this assay, the V626S mutant did not show a statistically significant growth advantage compared
340 to the parental strains. Nonetheless, it may still be a growth adaptive mutation based on
341 accumulated data (**Table 1, Fig 2**).

342 **Particle to infectious unit ratios for E2 mutants.** We next explored whether there
343 were functional differences in the properties of growth-adapted viruses compared to the parent
344 JFH-1 strain. We initially assessed the relative specific infectivity by measuring the RNA:$TCID_{50}$
345 ratio of each mutant virus (**Table 2**). A more efficient assembly process or increased stability of
346 infectious virions could contribute to increased peak titers. As HCV growth kinetic assays are
347 long, small differences may compound over time and account for at least part of the adaptive
348 growth phenotype. Using the tittered samples described in **Fig 2B**, viral RNA was harvested and
349 genome copy determined via RT-PCR using *in vitro* derived-RNA from infectious clone plasmids
350 as standards. The greatest difference between parent and a mutant virus was observed for
351 T563V, and even this fold-change was less than 4-fold. All mutant viruses, apart from K632T,
352 had a lower RNA:$TCID_{50}$ ratio than the parental virus, although these differences did not
353 achieve statistical significance.

354 **Buoyant density profiles of growth adapted mutants are similar to parent.** HCV has
355 a unique buoyant density profile when compared to many other *Flaviviridae* family members
356 (e.g., flaviviruses). Because of lipoprotein incorporation, infectious HCV particles have a lower
357 density and broader infectivity peak (3, 4). Some E2 growth variants have altered buoyant
358 density profiles relative to their parental strains (37, 40), and such differences may reflect
359 alterations in lipoprotein incorporation or changes to the subset of HCV particles (high or low
360 density) that display peak infectivity for a variant. To determine whether our panel of mutants

had shifts in buoyant density profiles, we performed sucrose gradient ultracentrifugation and quantified the density, viral titer, and HCV genome copy number in each fraction collected (**Fig 3**). The mutants all behaved similarly to parent virus, suggesting they have similar lipoprotein utilization or incorporation.

Some adaptive mutations enhance CD81-LEL and NMAb sensitivity. E2 is the major viral target of neutralizing antibodies during infection. Many of the most effective broadly NMAbs block interaction between E2 and CD81, one of the key HCV entry receptors (30, 31, 51, 52). Some growth-adaptive mutations in E2 were shown to increase inhibition by soluble CD81-LEL and NMAbs (37, 39, 40). To assess whether the identified mutations affected the binding of E2 to CD81, we performed inhibition of infection assays with a soluble CD81-LEL (**Fig 4A**). A subset of adaptive mutant viruses (T416R, T563V, and L619T) were inhibited more efficiently by CD81-LEL than the parent JFH-1 virus (>5-fold decrease in EC_{50}, $P < 0.05$), and thus an enhanced CD81-E2 interaction might contribute to the growth advantages of these viruses. However, most of the mutants were not more sensitive to CD81-LEL inhibition, which contrasts with some published growth-adaptive variants.

We next performed dose-response inhibition of infection assays with two broadly neutralizing anti-E2 NMAbs, H77.39 (**Fig 4B**) and HC84.26 (**Fig 4C**), both of which block interactions between E2 and CD81 (30, 31). H77.39 maps to an epitope centered on amino acids 415 and 417 and part of a larger epitope between positions 412-421. Residues within this region, especially W420, can influence CD81 interactions (24, 39). HC84.26 maps to conserved residues within the CD81 biding site between residues 441 and 446 and to residue 620 (H77 residue numbers). Q412R, T416R, S449P, T563V, and L619T viruses were neutralized more efficiently by H77.39 than the parent JFH1 (>5-fold decrease in EC_{50}, $P < 0.0001$) (**Fig 4B**) and T416R, S449P and T563V viruses were inhibited to a greater extent (>5-fold decrease in EC_{50}, $P < 0.05$) by HC84.26 (**Fig 4C**). However, A579R, V626S, K632T and L644I viruses were unchanged or exhibited modestly shifted profiles with anti-E2 NMAbs and CD81-LEL.

387 **HCV containing E2 adaptive mutations require CD81 and CLDN1 for infection.** HCV
388 entry is a complex process that requires several host factors including heparan sulfate
389 proteoglycans (53, 54), low-density lipoprotein receptor (54–56), SR-BI (21, 57), CD81 (51, 58),
390 CLDN1 (59), and occludin (OCLN) (60). Some E1 and E2 mutations cause altered entry factor
391 usage or reduce dependence on a particular receptor (37, 39, 40, 61). To test whether our
392 adaptive mutations changed CD81 or CLDN1 receptor dependency, we performed
393 neutralization assays with antibodies against these host entry factors. However, all of the
394 adaptive mutant viruses were inhibited by anti-CD81 and anti-CLDN1 similarly compared to the
395 parental strain, suggesting little change in dependency on these receptors (**Fig 5**).

396 **Growth-adaptive mutants are less-dependent on SR-BI for infection.** Markedly
397 different neutralization profiles were observed for the mutants when an anti-SR-BI antibody was
398 used (**Fig 6**), as each variant was more resistant to antibody inhibition. Whereas the parental
399 JFH-1 had a lower asymptote of 14% relative infection (i.e. resistant fraction), some mutant
400 viruses appeared to be entirely resistant to anti-SR-BI treatment of Huh7.5 cells. Even the most
401 sensitive mutant virus had a lower asymptote at 34% relative infection, 2.5-fold greater than
402 parent. To confirm changes to SR-BI dependency, we generated SR-BI^{KO} Huh7.5 cells using
403 CRISPR/Cas9 gene editing (**Fig 7**). A clonal SR-BI^{KO} Huh7.5 line, clone 16, was selected for
404 further study. Clone 16 was confirmed to lack SR-BI expression (**Fig 7A**) and exhibited a
405 moderately impaired capacity to support HCV cell entry (**Fig 7B**). Importantly, this phenotype
406 was restored completely by trans-complementation from a lentiviral vector (**Fig 7B**). Paired
407 infections of control (GFP) and SR-BI (SR-BI + GFP) trans-complemented SR-BI^{KO} cells with
408 WT and mutant HCV corroborated the anti-SR-BI antibody data: the mutants showed greater
409 infection in cells lacking SR-BI compared to the parental virus (**Fig 7C**). Thus, growth adaptation
410 in Huh7.5 cells resulted in the emergence of viruses with less dependency on SR-BI for
411 infection. To assess whether the mutations had a similar effect on other HCV genotypes, we
412 generated homologous mutations to JFH-1 S449P, L619T and L644I in a chimeric infectious

clone encoding the structural genes of the genotype 1 H77 isolate (H77/JFH-1). We performed paired infections of control and SR-BI trans-complemented SR-BI^{KO} cells with the H77/JFH-1 mutants and again observed less dependence on SR-BI for infection with the mutant viruses (**Fig 7D**). Finally, we explored whether deletion of SR-BI from Huh7.5 cells differentially affected the attachment of parent and mutant viruses. Notably, the attachment of all viruses to the SR-BI gene-edited cells was similar, suggesting the mutations likely affect a post-attachment interaction step that requires SR-BI (**Fig 7E**).

Our results suggested that all of the growth adaptive mutations identified in our screen modulated the SR-BI dependence of HCV for entry into target cells. When we mapped the positions of the growth adaptive mutations on the E2 core structure (19), we found that four of the residues (L619T, V626S and K632T, and L644I) were proximal to one another, with K632T, and L644I directly adjacent in an anti-parallel beta hairpin (**Fig 7F**). This clustering suggests a possible role for this region of E2 in an interaction with SR-BI.

DISCUSSION

The study of single amino acid viral variants has facilitated advances in our understanding of host-pathogen interactions. However, classical methods of producing viral variants rely on stochastic errors of the viral polymerase to generate mutations. Such approaches can be an inefficient means of producing new mutants even when selective pressure is applied. This approach may fail to explore all possible amino acid substitutions, as multiple nucleotide changes at a single codon are less likely. The limitation of relying on randomly occurring mutations is particularly problematic for HCV, as it is relatively slow growing in culture. By molecularly engineering variability into E2 and producing our SDSM library we circumvented the need to wait months for mutations to arise in culture. Where previous attempts to identify new culture adaptive mutations yielded few mutations, we selected for many variants within three tissue culture passages.

Previous studies of growth-enhancing E2 mutations were limited to a few sites with E2, between positions 412-421 and at positions 451 and 563 (38–41). These mutations increased the sensitivity of the virus to inhibition by CD81-LEL and anti-HCV NMAbs targeting the E2-CD81 interaction. These mutations may elicit a more open E2 conformation, which promotes interactions with CD81 or other entry factors at the cost of greater exposure of the NMAbs that block access to the CD81 binding site on E2. Additionally, some of these prior mutations altered the dependence of HCV on SR-BI and caused a shift in the buoyant density profile of the infectious viruses. In comparison, our panel of mutations were distributed more evenly across the E2 protein. Four substitutions (Q412R, T416R, S449P and T563V) were proximal to the previously described positions, however the remaining five mutations (A579R, L619T, V626S, K632T, and L644I) were at unique positions within E2.

The increased sensitivity to NMAb and CD81-LEL inhibition by growth-enhancing E2 mutations may represent a trade-off made by the virus in the face of humoral immune pressure, with a compromise of growth kinetics to facilitate immune evasion. Consistent with this

452 hypothesis, an alignment of all genotype 2 E2 amino acid sequences in the ViPR database
453 (http://www.viprbrc.org/) revealed that our adaptive mutations were present at low frequencies
454 or absent from most HCV isolates (**Table 3**). A subset of our mutations, Q412R, T416R, S449P,
455 T563V, and L619T, were more sensitive to NMAb inhibition than the parental virus. Of these,
456 T416R, T563V and L619T also were more sensitive to inhibition by CD81-LEL. T416R falls
457 within the epitope of H77.39 and correspondingly is neutralized more efficiently by this antibody.
458 The S449P mutation eliminates a predicted N-linked glycosylation site at N448 near the CD81
459 binding site, which might enhance NMAb potency by reducing steric hindrance of the glycan. At
460 present, the effects of other residues on the potency of neutralization by H77.39 and HC84.26
461 are more challenging to model. Structural data for the binding of these antibodies to E2 are not
462 available, and some of the residues are not visible in the crystal structures of the E2 core.
463 Residues that are not proximal to the footprints of H77.39 and HC84.26 could affect
464 neutralization potency indirectly, perhaps via altered lipoprotein association or changes in the
465 global conformation of E2.

466 Q412R and S449P were more sensitive to H77.39 and HC84.26 antibody neutralization
467 without showing increased inhibition by CD81-LEL. This suggests that increased exposure of
468 the CD81 binding site is not responsible exclusively for enhanced anti-E2 neutralization. We
469 also identified growth adaptive mutations in E2 (e.g., A579R and K632T) that did not render the
470 virus more susceptible to neutralizing antibodies, although further studies are warranted. These
471 mutants could be more sensitive to NMAbs targeting different epitopes. Alternatively, these
472 mutations may adapt the virus to Huh7.5 cells but not to cell targets *in vivo.*

473 Mutations in E1 and E2 can alter the dependence of HCV on particular receptors or even
474 cause a shift in receptor utilization (37, 39, 40, 61). We tested whether our growth adapted
475 viruses had different entry factor utilization. Antibodies to CD81 and CLDN1 showed little
476 difference in potency between the mutant and parental viruses; thus, the mutant viruses
477 remained dependent on CD81 and CLDN1 for entry. A different pattern was observed when

478 cells were pretreated with anti-SR-BI antibodies. Parental virus was neutralized efficiently with a
479 90% reduction at high antibody concentrations. However, all of the growth adapted viruses were
480 resistant to the effects of anti-SR-BI, a finding which was corroborated using CRISPR/Cas9
481 generated SR-BI^{KO} and trans-complemented cells. Additionally, H77/JFH-1 clones bearing
482 homologous mutations to JFH-1 S449P, L619T and L644I, similarly were resistant to SR-BI
483 deletion, suggesting the mutations have a conserved role in modulating the SR-BI interaction.
484 As changes to lipoprotein incorporation could contribute to the observed SR-BI phenotype of
485 some growth adaptive mutants, we analyzed buoyant density profiles for relative infectivity.
486 However, all of our growth adaptive mutants had virtually identical profiles relative to parental
487 virus. This observation suggests that the altered SR-BI usage may not be a function of changes
488 to lipoprotein incorporation. Consistent with this idea, HCV uses SR-BI at multiple points in the
489 entry pathway, as an attachment factor via interactions with virus associated lipoprotein and
490 also during post-attachment steps by directly interacting with E2 (62). As deletion of SR-BI did
491 not differentially affect attachment of parent or variant HCV to Huh7.5 cells, these mutations
492 may alter a post-attachment interaction with SR-BI.

493 While it is known that deletion of HVR1 abrogates binding of E2 to SR-BI, the details of
494 this interaction remain unclear. Our findings, along with data from previous studies, suggest that
495 reduced SR-BI dependence for infection is a common feature of growth-enhancing E2
496 mutations (at least in cell culture) and that residues distributed across the E2 protein can
497 modulate the interaction with SR-BI. As four of the sites of growth adaptive mutations we
498 identified with altered SR-BI dependency were proximal to each other, we speculate this could
499 represent part of a possible SR-BI binding site in E2. The molecular basis for why our mutants
500 show less dependency on SR-BI awaits more detailed structural or biochemical resolution of the
501 E2 and SR-BI interaction.

502 In summary, we developed a novel E2 JFH-1 mutant library with significant diversity and
503 used it to identify new growth adaptive mutations for study. The properties of these mutants are

summarized in **Table 4**, and varied with respect to NMAb and CD81-LEL inhibition sensitivity and SR-BI-dependence. More broadly, these results demonstrate the utility of libraries of variant viruses to address questions in HCV biology, especially as it relates to receptor interactions and possibly, immune escape. The SDSM method provides a depth of variability that can be employed rapidly for discovery of novel HCV variants with unique functional profiles.

ACKNOWLEDGEMENTS

We thank the Genome Technology Access Center in the Department of Genetics at Washington University School of Medicine for help with genomic analysis. The Center is partially supported by NCI Cancer Center Support Grant (P30 CA91842) to the Siteman Cancer Center and by ICTS/CTSA (UL1 TR000448) from the National Center for Research Resources (NCRR), a component of the National Institutes of Health (NIH), and NIH Roadmap for Medical Research. M.J.E was supported by the National Institutes of Health/National Institute of Diabetes and Digestive and Kidney Diseases (R01 DK095125), the American Cancer Society (RSG-12-176-01-MPC), the Pew Charitable Funds, and Burroughs Wellcome Fund.

520 **REFERENCES**

521 1. **Mohd Hanafiah K**, **Groeger J**, **Flaxman AD**, **Wiersma ST**. 2013. Global epidemiology of
522 hepatitis C virus infection: new estimates of age-specific antibody to HCV
523 seroprevalence. Hepatology **57**:1333–42.

524 2. **Hajarizadeh B**, **Grebely J**, **Dore GJ**. 2013. Epidemiology and natural history of HCV
525 infection. Nat. Rev. Gastroenterol. Hepatol. **10**:553–62.

526 3. **Thomssen R**, **Bonk S**, **Propfe C**, **Heermann KH**, **Köchel HG**, **Uy A**. 1992. Association
527 of hepatitis C virus in human sera with beta-lipoprotein. Med. Microbiol. Immunol.
528 **181**:293–300.

529 4. **Nielsen SU**, **Bassendine MF**, **Burt AD**, **Martin C**, **Pumeechockchai W**, **Geoffrey L**,
530 **Toms GL**. 2006. Association between Hepatitis C Virus and Very-Low-Density
531 Lipoprotein (VLDL)/ LDL Analyzed in Iodixanol Density Gradients Association between
532 Hepatitis C Virus and Very-Low-Density Lipoprotein (VLDL)/ LDL Analyzed in Iodixanol
533 Density Gradients. J. Virol. **80**:2418–2428.

534 5. **Smith DB**, **Bukh J**, **Kuiken C**, **Muerhoff AS**, **Rice CM**, **Stapleton JT**, **Simmonds P**.
535 2013. Expanded classification of hepatitis C Virus into 7 genotypes and 67 Subtypes:
536 updated criteria and assignment web resource. Hepatology DOI: 10.1002/hep.26744.

537 6. **Saeed M**, **Andreo U**, **Chung H-Y**, **Espiritu C**, **Branch AD**, **Silva JM**, **Rice CM**. 2015.
538 SEC14L2 enables pan-genotype HCV replication in cell culture. Nature **524**:471–5.

539 7. **Zhong J**, **Gastaminza P**, **Cheng G**, **Kapadia S**, **Kato T**, **Burton DR**, **Wieland SF**,
540 **Uprichard SL**, **Wakita T**, **Chisari F V**. 2005. Robust hepatitis C virus infection in vitro.
541 Proc. Natl. Acad. Sci. U. S. A. **102**:9294–9.

542 8. **Wakita T**, **Pietschmann T**, **Kato T**, **Date T**, **Miyamoto M**, **Zhao Z**, **Murthy K**,
543 **Habermann A**, **Kräusslich H-G**, **Mizokami M**, **Bartenschlager R**, **Liang TJ**. 2005.
544 Production of infectious hepatitis C virus in tissue culture from a cloned viral genome.
545 Nat. Med. **11**:791–6.

9. **Lindenbach BD**, **Evans MJ**, **Syder AJ**, **Wölk B**, **Tellinghuisen TL**, **Liu CC**, **Maruyama T**, **Hynes RO**, **Burton DR**, **McKeating JA**, **Rice CM**. 2005. Complete replication of hepatitis C virus in cell culture. Science **309**:623–6.

10. **Li Y-P**, **Ramirez S**, **Jensen SB**, **Purcell RH**, **Gottwein JM**, **Bukh J**. 2012. Highly efficient full-length hepatitis C virus genotype 1 (strain TN) infectious culture system. Proc. Natl. Acad. Sci. U. S. A. **109**:19757–62.

11. **Li Y-P**, **Ramirez S**, **Gottwein JM**, **Scheel TKH**, **Mikkelsen L**, **Purcell RH**, **Bukh J**. 2012. Robust full-length hepatitis C virus genotype 2a and 2b infectious cultures using mutations identified by a systematic approach applicable to patient strains. Proc. Natl. Acad. Sci. U. S. A. **109**:E1101–10.

12. **Li Y-P**, **Ramirez S**, **Mikkelsen L**, **Bukh J**. 2015. Efficient Infectious Cell Culture Systems of the Hepatitis C Virus (HCV) Prototype Strains HCV-1 and H77. J. Virol. **89**:811–823.

13. **Kim S**, **Date T**, **Yokokawa H**, **Kono T**, **Aizaki H**, **Maurel P**, **Gondeau C**, **Wakita T**. 2014. Development of hepatitis C virus genotype 3a cell culture system. Hepatology **60**:1838–50.

14. **Farci P**, **Shimoda A**, **Coiana A**, **Diaz G**, **Peddis G**, **Melpolder JC**, **Strazzera A**, **Chien DY**, **Munoz SJ**, **Balestrieri A**, **Purcell RH**, **Alter HJ**. 2000. The outcome of acute hepatitis C predicted by the evolution of the viral quasispecies. Science **288**:339–44.

15. **Liu L**, **Fisher BE**, **Dowd KA**, **Astemborski J**, **Cox AL**, **Ray SC**. 2010. Acceleration of hepatitis C virus envelope evolution in humans is consistent with progressive humoral immune selection during the transition from acute to chronic infection. J. Virol. **84**:5067–77.

16. **Lindenbach BD**, **Rice CM**. 2013. The ins and outs of hepatitis C virus entry and assembly. Nat. Rev. Microbiol. **11**:688–700.

17. **Falson P**, **Bartosch B**, **Alsaleh K**, **Tews BA**, **Loquet A**, **Ciczora Y**, **Riva L**, **Montigny C**, **Montpellier C**, **Duverlie G**, **Pécheur E-I**, **le Maire M**, **Cosset F-L**, **Dubuisson J**,

Penin F. 2015. Hepatitis C Virus Envelope Glycoprotein E1 Forms Trimers at the Surface of the Virion. J. Virol. **89**:10333–46.

18. **Vieyres G**, **Thomas X**, **Descamps V**, **Duverlie G**, **Patel AH**, **Dubuisson J**. 2010. Characterization of the envelope glycoproteins associated with infectious hepatitis C virus. J. Virol. **84**:10159–68.

19. **Kong L**, **Giang E**, **Nieusma T**, **Kadam RU**, **Cogburn KE**, **Hua Y**, **Dai X**, **Stanfield RL**, **Burton DR**, **Ward AB**, **Wilson IA**, **Law M**. 2013. Hepatitis C virus E2 envelope glycoprotein core structure. Science **342**:1090–4.

20. **Khan AG**, **Whidby J**, **Miller MT**, **Scarborough H**, **Zatorski A V**, **Cygan A**, **Price AA**, **Yost SA**, **Bohannon CD**, **Jacob J**, **Grakoui A**, **Marcotrigiano J**. 2014. Structure of the core ectodomain of the hepatitis C virus envelope glycoprotein 2. Nature **509**:381–4.

21. **Scarselli E**, **Ansuini H**, **Cerino R**, **Roccasecca RM**, **Acali S**, **Filocamo G**, **Traboni C**, **Nicosia A**, **Cortese R**, **Vitelli A**. 2002. The human scavenger receptor class B type I is a novel candidate receptor for the hepatitis C virus. EMBO J. **21**:5017–25.

22. **Bankwitz D**, **Steinmann E**, **Bitzegeio J**, **Ciesek S**, **Friesland M**, **Herrmann E**, **Zeisel MB**, **Baumert TF**, **Keck Z**, **Foung SKH**, **Pécheur E-I**, **Pietschmann T**. 2010. Hepatitis C virus hypervariable region 1 modulates receptor interactions, conceals the CD81 binding site, and protects conserved neutralizing epitopes. J. Virol. **84**:5751–63.

23. **Drummer HE**, **Boo I**, **Maerz AL**, **Poumbourios P**. 2006. A conserved Gly436-Trp-Leu-Ala-Gly-Leu-Phe-Tyr motif in hepatitis C virus glycoprotein E2 is a determinant of CD81 binding and viral entry. J. Virol. **80**:7844–53.

24. **Owsianka AM**, **Timms JM**, **Tarr AW**, **Brown RJP**, **Hickling TP**, **Szwejk A**, **Bienkowska-Szewczyk K**, **Thomson BJ**, **Patel AH**, **Ball JK**. 2006. Identification of conserved residues in the E2 envelope glycoprotein of the hepatitis C virus that are critical for CD81 binding. J. Virol. **80**:8695–704.

25. **Jiang J**, **Luo G**. 2012. Cell culture-adaptive mutations promote viral protein-protein

interactions and morphogenesis of infectious hepatitis C virus. J. Virol. **86**:8987–97.

26. **Kato T**, **Furusaka A**, **Miyamoto M**, **Date T**, **Yasui K**, **Hiramoto J**, **Nagayama K**, **Tanaka T**, **Wakita T**. 2001. Sequence analysis of hepatitis C virus isolated from a fulminant hepatitis patient. J. Med. Virol. **64**:334–9.

27. **Reed LJ**, **Muench H**. 1938. A Simple Method of Estimating Fifty Per Cent Endpoints. Am. J. Hyg. **27**:493–497.

28. **Yi M**, **Ma Y**, **Yates J**, **Lemon SM**. 2007. Compensatory mutations in E1, p7, NS2, and NS3 enhance yields of cell culture-infectious intergenotypic chimeric hepatitis C virus. J. Virol. **81**:629–38.

29. **Pickett BE**, **Sadat EL**, **Zhang Y**, **Noronha JM**, **Squires RB**, **Hunt V**, **Liu M**, **Kumar S**, **Zaremba S**, **Gu Z**, **Zhou L**, **Larson CN**, **Dietrich J**, **Klem EB**, **Scheuermann RH**. 2012. ViPR: An open bioinformatics database and analysis resource for virology research. Nucleic Acids Res. **40**:593–598.

30. **Keck Z**, **Xia J**, **Wang Y**, **Wang W**, **Krey T**, **Prentoe J**, **Carlsen T**, **Li AY-J**, **Patel AH**, **Lemon SM**, **Bukh J**, **Rey FA**, **Foung SKH**. 2012. Human monoclonal antibodies to a novel cluster of conformational epitopes on HCV E2 with resistance to neutralization escape in a genotype 2a isolate. PLoS Pathog. **8**:e1002653.

31. **Sabo MC**, **Luca VC**, **Prentoe J**, **Hopcraft SE**, **Blight KJ**, **Yi M**, **Lemon SM**, **Ball JK**, **Bukh J**, **Evans MJ**, **Fremont DH**, **Diamond MS**. 2011. Neutralizing monoclonal antibodies against hepatitis C virus E2 protein bind discontinuous epitopes and inhibit infection at a postattachment step. J. Virol. **85**:7005–19.

32. **Nelson CA**, **Lee CA**, **Fremont DH**. 2014. Oxidative refolding from inclusion bodies. Methods Mol. Biol. **1140**:145–157.

33. **Meuleman P**, **Catanese MT**, **Verhoye L**, **Desombere I**, **Farhoudi A**, **Jones CT**, **Sheahan T**, **Grzyb K**, **Cortese R**, **Rice CM**, **Leroux-Roels G**, **Nicosia A**. 2012. A human monoclonal antibody targeting scavenger receptor class B type I precludes

hepatitis C virus infection and viral spread in vitro and in vivo. Hepatology **55**:364–72.

34. **Hötzel I**, **Chiang V**, **Diao J**, **Pantua H**, **Maun HR**, **Kapadia SB**. 2011. Efficient production of antibodies against a mammalian integral membrane protein by phage display. Protein Eng. Des. Sel. **24**:679–89.

35. **Mali P**, **Yang L**, **Esvelt KM**, **Aach J**, **Guell M**, **DiCarlo JE**, **Norville JE**, **Church GM**. 2013. RNA-guided human genome engineering via Cas9. Science (80-.). **339**:823–826.

36. **Michta ML**, **Hopcraft SE**, **Narbus CM**, **Kratovac Z**, **Israelow B**, **Sourisseau M**, **Evans MJ**. 2010. Species-specific regions of occludin required by hepatitis C virus for cell entry. J. Virol. **84**:11696–11708.

37. **Grove J**, **Nielsen S**, **Zhong J**, **Bassendine MF**, **Drummer HE**, **Balfe P**, **McKeating JA**. 2008. Identification of a residue in hepatitis C virus E2 glycoprotein that determines scavenger receptor BI and CD81 receptor dependency and sensitivity to neutralizing antibodies. J. Virol. **82**:12020–9.

38. **Zhong J**, **Gastaminza P**, **Chung J**, **Stamataki Z**, **Isogawa M**, **Cheng G**, **McKeating JA**, **Chisari F V**. 2006. Persistent hepatitis C virus infection in vitro: coevolution of virus and host. J. Virol. **80**:11082–93.

39. **Dhillon S**, **Witteveldt J**, **Gatherer D**, **Owsianka AM**, **Zeisel MB**, **Zahid MN**, **Rychłowska M**, **Foung SKH**, **Baumert TF**, **Angus AGN**, **Patel AH**. 2010. Mutations within a conserved region of the hepatitis C virus E2 glycoprotein that influence virus-receptor interactions and sensitivity to neutralizing antibodies. J. Virol. **84**:5494–507.

40. **Tao W**, **Xu C**, **Ding Q**, **Li R**, **Xiang Y**, **Chung J**, **Zhong J**. 2009. A single point mutation in E2 enhances hepatitis C virus infectivity and alters lipoprotein association of viral particles. Virology **395**:67–76.

41. **Kim CS**, **Keum SJ**, **Jang SK**. 2011. Generation of a cell culture-adapted hepatitis C virus with longer half life at physiological temperature. PLoS One **6**:e22808.

42. **Kaul A**, **Woerz I**, **Meuleman P**, **Leroux-Roels G**, **Bartenschlager R**. 2007. Cell culture

adaptation of hepatitis C virus and in vivo viability of an adapted variant. J. Virol. **81**:13168–79.

43. **Russell RS**, **Meunier J-C**, **Takikawa S**, **Faulk K**, **Engle RE**, **Bukh J**, **Purcell RH**, **Emerson SU**. 2008. Advantages of a single-cycle production assay to study cell culture-adaptive mutations of hepatitis C virus. Proc. Natl. Acad. Sci. U. S. A. **105**:4370–5.

44. **Sabahi A**, **Uprichard SL**, **Wimley WC**, **Dash S**, **Garry RF**. 2014. Unexpected structural features of the hepatitis C virus envelope protein 2 ectodomain. J. Virol. **88**:10280–8.

45. **Song H**, **Ren F**, **Li J**, **Shi S**, **Yan L**, **Gao F**, **Li K**, **Zhuang H**. 2012. A laboratory-adapted HCV JFH-1 strain is sensitive to neutralization and can gradually escape under the selection pressure of neutralizing human plasma. Virus Res. **169**:154–161.

46. **Bungyoku Y**, **Shoji I**, **Makine T**, **Adachi T**, **Hayashida K**, **Nagano-Fujii M**, **Ide Y-H**, **Deng L**, **Hotta H**. 2009. Efficient production of infectious hepatitis C virus with adaptive mutations in cultured hepatoma cells. J. Gen. Virol. **90**:1681–91.

47. **Kang J-I**, **Kim JP**, **Wakita T**, **Ahn B-Y**. 2009. Cell culture-adaptive mutations in the NS5B gene of hepatitis C virus with delayed replication and reduced cytotoxicity. Virus Res. **144**:107–16.

48. **Pokrovskii M V**, **Bush CO**, **Beran RKF**, **Robinson MF**, **Cheng G**, **Tirunagari N**, **Fenaux M**, **Greenstein AE**, **Zhong W**, **Delaney WE**, **Paulson MS**. 2011. Novel mutations in a tissue culture-adapted hepatitis C virus strain improve infectious-virus stability and markedly enhance infection kinetics. J. Virol. **85**:3978–85.

49. **Liu S**, **Xiao L**, **Nelson C**, **Hagedorn CH**, **Hagedorn C**. 2012. A cell culture adapted HCV JFH1 variant that increases viral titers and permits the production of high titer infectious chimeric reporter viruses. PLoS One **7**:e44965.

50. **Aligeti M**, **Roder A**, **Horner SM**. 2015. Cooperation between the Hepatitis C Virus p7 and NS5B Proteins Enhances Virion Infectivity. J. Virol. **89**:11523–33.

51. **Pileri P**, **Uematsu Y**, **Campagnoli S**, **Galli G**. 1998. Binding of hepatitis C virus to CD81.

Science (80-.). **282**:938–941.

52. **Law M**, **Maruyama T**, **Lewis J**, **Giang E**, **Tarr AW**, **Stamataki Z**, **Gastaminza P**, **Chisari F V**, **Jones IM**, **Fox RI**, **Ball JK**, **McKeating JA**, **Kneteman NM**, **Burton DR**. 2008. Broadly neutralizing antibodies protect against hepatitis C virus quasispecies challenge. Nat. Med. **14**:25–7.

53. **Barth H**, **Schafer C**, **Adah MI**, **Zhang F**, **Linhardt RJ**, **Toyoda H**, **Kinoshita-Toyoda A**, **Toida T**, **Van Kuppevelt TH**, **Depla E**, **Von Weizsacker F**, **Blum HE**, **Baumert TF**. 2003. Cellular binding of hepatitis C virus envelope glycoprotein E2 requires cell surface heparan sulfate. J. Biol. Chem. **278**:41003–12.

54. **Germi R**, **Crance J-M**, **Garin D**, **Guimet J**, **Lortat-Jacob H**, **Ruigrok RWH**, **Zarski J-P**, **Drouet E**. 2002. Cellular glycosaminoglycans and low density lipoprotein receptor are involved in hepatitis C virus adsorption. J. Med. Virol. **68**:206–215.

55. **Monazahian M**, **Böhme I**, **Bonk S**, **Koch A**, **Scholz C**, **Grethe S**, **Thomssen R**. 1999. Low density lipoprotein receptor as a candidate receptor for hepatitis C virus. J. Med. Virol. **57**:223–229.

56. **Agnello V**, **Abel G**, **Elfahal M**, **Knight GB**, **Zhang QX**. 1999. Hepatitis C virus and other flaviviridae viruses enter cells via low density lipoprotein receptor. Proc. Natl. Acad. Sci. U. S. A. **96**:12766–71.

57. **Bartosch B**, **Vitelli A**, **Granier C**, **Goujon C**, **Dubuisson J**, **Pascale S**, **Scarselli E**, **Cortese R**, **Nicosia A**, **Cosset F-L**. 2003. Cell entry of hepatitis C virus requires a set of co-receptors that include the CD81 tetraspanin and the SR-B1 scavenger receptor. J. Biol. Chem. **278**:41624–30.

58. **Flint M**, **Maidens C**, **Loomis-price LD**, **Shotton C**, **Dubuisson J**, **Monk P**, **Higginbottom A**, **Levy S**, **Mckeating JA**. 1999. Characterization of Hepatitis C Virus E2 Glycoprotein Interaction with a Putative Cellular Receptor, CD81. J. Virol. **73(8)**:6235–6244.

59. **Evans MJ**, **von Hahn T**, **Tscherne DM**, **Syder AJ**, **Panis M**, **Wölk B**, **Hatziioannou T**, **McKeating JA**, **Bieniasz PD**, **Rice CM**. 2007. Claudin-1 is a hepatitis C virus co-receptor required for a late step in entry. Nature **446**:801–5.

60. **Ploss A**, **Evans MJ**, **Gaysinskaya VA**, **Panis M**, **You H**, **de Jong YP**, **Rice CM**. 2009. Human occludin is a hepatitis C virus entry factor required for infection of mouse cells. Nature **457**:882–6.

61. **Hopcraft SE**, **Evans MJ**. 2015. Selection of a hepatitis C virus with altered entry factor requirements reveals a genetic interaction between the E1 glycoprotein and claudins. Hepatology **62 (4)**:1059–1069.

62. **Dao Thi VL**, **Granier C**, **Zeisel MB**, **Guérin M**, **Mancip J**, **Granio O**, **Penin F**, **Lavillette D**, **Bartenschlager R**, **Baumert TF**, **Cosset F-L**, **Dreux M**. 2012. Characterization of hepatitis C virus particle subpopulations reveals multiple usage of the scavenger receptor BI for entry steps. J. Biol. Chem. **287**:31242–57.

716 **FIGURE LEGENDS**

717 **Figure 1. Generation of a SDSM library of infectious HCV and selection of growth**
718 **adaptive mutations. A.** Summary of the strategy used to generate the SDSM E2 library. Three-
719 hundred and twenty degenerate (NNN) primer sets were used to randomize each codon in the
720 ectodomain of E2, excluding cysteine residues. These plasmid libraries were grouped into sets
721 of 10 sequential codons. E1-E2 fragments amplified by PCR from these plasmid pools were
722 used to generate 32 pools of mutant viruses. **B**. Amplicon sequencing results for the plasmid
723 libraries. The frequency of mutant codons at each position within the library is shown. The ideal
724 mutant frequency is 10% using our approach (red dashed line).

725 **Figure 2. Growth kinetics of viruses bearing the dominant mutations identified by**
726 **serial passage of E2 mutant pools. A**. Huh7.5 cells were infected with each of the nine
727 mutants selected for study and parent virus at a MOI of 0.1 based on titers calculated using the
728 $TCID_{50}$ method. Input virus was removed 6 h after infection and samples collected every 24 h for
729 7 days. Supernatant viral titers were analyzed by FFA. **B.** Cultures of Huh7.5 cells were infected
730 as in (**A**) at a MOI of 0.05. Inoculum (black bars) and titers of virus from supernatant at day 5
731 (grey bars) were determined using the $TCID_{50}$ method. Error bars represent standard error of
732 the mean (SEM) and dashed lines indicate the limit of detection of the assays. Asterisks indicate
733 differences that are statistically significant (*, $P < 0.05$; **, $P < 0.01$; ***, $P < 0.001$; ****, $P <$
734 0.0001; ns, not significant). The results are the average of three independent experiments
735 performed in duplicate.

736 **Figure 3. Growth enhancing mutations do not change buoyant density profiles.**
737 Virus-containing media was layered over 5-50% sucrose gradients and ultracentrifuged at
738 105,000 x g for 17 hours at 4°C. Twelve 1 mL fractions were collected. The density of the liquid
739 in each fraction was determined using a refractometer, and viral titers and genome copies in
740 each fraction were quantified by FFA and RT-PCR, respectively. In each panel, the percent of
741 total infectious virus collected in each fraction is displayed in the top graph and the percent of

742 total genome copies in the bottom, with a control plot for the parental virus shown in red. The
743 mutants are displayed in the panels as follows: Q412R (**A**); T416R (**B**); S449P (**C**); T563V (**D**);
744 A579R (**E**); L619T (**F**); V626S (**G**); K632T (**H**); and L644I (**I**). Panel (**J**) includes a comparison
745 between parent JFH-1, the T416R mutant and J6/JFH-1 viruses run as a control to confirm
746 differences in buoyant density profiles could be measured using our experimental approach.
747 Each point represents the mean of three independent experiments with error bars representing
748 SEM.

749 **Figure 4. A subset of growth enhanced mutants are more sensitive to CD81-LEL**
750 **and NMAb inhibition.** Parental or mutant viruses were pre-incubated with a dilution series of
751 CD81-LEL (**A**) or anti-E2 antibodies H77.39 (**B**) or HC84.26 (**C**) for 1 h at 37°C and then added
752 to Huh7.5 cells. Infection was quantified 72 h later by FFA. EC_{50} values were determined by
753 non-linear regression analysis. The left panels are representative dose response curves for
754 parental virus and the mutants. The fold decrease in EC_{50} value for the antibody treatment
755 relative to parental virus is plotted in the right panel. Asterisks indicate differences that are
756 statistically significant (*, $P < 0.05$; **, $P < 0.01$; ***, $P < 0.001$; ****, $P < 0.0001$; ns, not
757 significant). Error bars represent SEM. The results are the average of three independent
758 experiments performed in triplicate or quadruplicate.

759 **Figure 5. The dependence on CD81 and CLDN1 for growth adapted mutants is**
760 **similar to the parental virus.** Huh7.5 cells were pre-incubated with a dilution series of anti-
761 CD81 (**A**) or anti-CLDN1 (**B**) for 1 h at 37°C and then infected with parental and growth adapted
762 mutant viruses. Infection was quantified 72 h later by FFA and EC_{50} values determined by non-
763 linear regression. For each mutant virus, the fold change in EC_{50} value for the antibody
764 treatment relative to parental virus is plotted. Asterisks indicate differences that are statistically
765 significant (*, $P < 0.05$; **, $P < 0.01$; ns, not significant). Error bars represent SEM. The results
766 are the average of three independent experiments performed in triplicate or quadruplicate.

767 **Figure 6. Growth enhanced mutants are less dependent on SR-BI for infection.**
768 Huh7.5 cells were pre-incubated with a dilution series of anti-SR-BI for 1 h at 37°C and then
769 infected with parental and mutant viruses. Infection was quantified 72 h later by FFA. In each
770 panel, the dose-response curve for a single mutant virus is displayed with the same control
771 dose-response curve for parental virus. The mutants are displayed in the panels as follows:
772 Q412R (**A**); T416R (**B**); S449P (**C**); T563V (**D**); A579R (**E**); L619T (**F**); V626S (**G**); K632T (**H**);
773 and L644I (**I**). Error bars represent SEM. The results are the average of three independent
774 experiments performed in quadruplicate

775 **Figure 7. Generation of SR-BI deficient Huh7.5 cells. A.** Parental Huh7.5 cells or
776 Huh7.5 SR-BI^{KO} clone cell populations were stained with isotype control or SR-BI specific
777 antibodies and analyzed by flow cytometry. **B.** The relative titers of a single stock of HCV were
778 determined by limiting dilution assay on parental Huh7.5 cells or Huh7.5 SR-BI^{KO} clonal cells
779 either not expressing a transgene ('mock') or transduced with lentiviral particles to express GFP
780 or SR-BI. Values represent the mean $TCID_{50}$/mL value and the error bars indicate SEM of three
781 independent assays. **C.** SR-BI^{KO} Huh7.5 cells stably expressing GFP or GFP and SR-BI were
782 infected with parental or variant virus. The relative infection of GFP-only cells compared to GFP
783 and SR-BI co-expressing cells is shown. Error bars represent SEM. Asterisks indicate
784 differences that are statistically significant (*, $P < 0.05$; ***, $P < 0.001$; ****, $P < 0.0001$). The
785 results are the average of three independent experiments performed in quadruplicate. **D.** SR-
786 BI^{KO} Huh7.5 cells stably expressing GFP or GFP and SR-BI were infected as described in (**C**)
787 using parental H77/JFH-1 and H77/JFH-1 variant viruses bearing corresponding mutations to
788 JFH-1 S449P, L619T, and L644: S449P, L615T and L640L, respectively. **E.** SR-BI^{KO} Huh7.5
789 cells stably expressing GFP or GFP and SRBI were incubated with parental or variant virus or 3
790 h on ice. Cells were washed extensively, cellular RNA was harvested, and HCV genome copies
791 were quantified by qRT-PCR. The relative attachment to GFP-only cells compared to GFP and
792 SR-BI co-expressing cells is shown. Error bars represent SEM. No statistically significant

differences were observed. The results are the average of three independent experiments performed in duplicate. **F.** Ribbon diagram of the E2 core structure (PDB ID: 4MWF) (19) illustrating the locations of the adaptive mutations identified in this study (red spheres) and residues essential for CD81 binding (blue spheres, amino acid positions 529-535). Q412 and T416 were excluded as they fall within a disordered region.

799 **Table 1: Mutations selected by serial passage of HCV E2 mutant pools**

Positions of mutations in E2 of P0 virus	Positions of P3 putative adaptive mutations identified by consensus sequencing	Amino acid substitutions identified by colony sequencing (% of colonies bearing the substitution)	Other sites of mutations identified by colony sequencing
404-413	Q412	R (33%), A (11%), D (3%)	I411, L413
414-423	T416	R (16%), K (10%), N (5%), V (5%), A (5%), G (3%), D (3%)	I414, N415, N417, G418
445-455	S449	No Data*	
562-573	T563	V (33%), L (33%), I (2%)	T565
574-583	A579	R (17%), L (10%), M (7%)	
618-628	L619	T (34%), E (9%), I (2%)	W620
	V626	S (15%), T (2%), Q (2%), E (2%), R (2%)	
629-638	K632	T (62%)	I630
639-649	L644	I (32%), V (14%)	A646

800 * Consensus sequencing suggested only a proline substitution.

801 Each pool of E2 mutants was passaged three times in tissue culture. Subsequently, viral RNA
802 was harvested, cDNA generated, and E1-E2 amplified by PCR and Sanger sequenced across
803 the sites of engineered mutations within E2. Eight of the thirty-two pools had changes to the E2
804 consensus sequence: 404-413, 414-423, 445-455, 563-573, 574-583, 618-628, 629-638, and
805 639-649. The E1-E2 fragments from these samples were cloned, and plasmids from individual
806 colonies were sequenced to determine the specific amino acid substitutions selected from each
807 pool.

808

809 **Table 2: Genome copy number to $TCID_{50}$ ratios for growth enhanced mutants**

Virus	Parent	Q412R	T416R	S449P	T563V	A579R	L619T	V626S	K632T	L644I
Genome Copy per $TCID_{50}$	$7.1x10^3$	$3.5 x10^3$	$2.7 x10^3$	$3.2 x10^3$	$1.9 x10^3$	$2.4 x10^3$	$2.4 x10^3$	$3.9 x10^3$	$6.3 x10^3$	$4.7 x10^3$
Fold-decrease relative to parent	-	2.0	2.7	2.2	3.8	2.9	2.9	1.8	1.1	1.5

810

811 Huh7.5 cell cultures were infected at a MOI of 0.05 with each mutant and the parental virus. The
812 inoculum was washed off and 5 days post infection nascently produced virus was collected and
813 titered by the $TCID_{50}$ method. Genome copies were measured by RT-PCR. Values are the
814 mean of three experiments performed in duplicate.

815

816 **Table 3: Number of genotype 2 sequences in the ViPR database bearing each amino acid**
817 **at the site of adaptive mutation.**

	Q412R	T416R	S449P	T563V	A579R	L619T	V626S	K632T	L644I
Ala (A)	4	33	1338	1	**252**				
Arg (R)	**31**		1		**9**			1	
Asn (N)	136	82	1						
Asp (D)	13	2	212						
Cys (C)							1		
Gln (Q)	**3986**		1		1			4	
Glu (E)	181	110	2		1				
Gly (G)	9		3		11			1	
His(H)	36		1		3				
Ile (I)	2			1			7		**1**
Leu (L)	4		117			**469**	9		**417**
Lys (K)	5	8	4					**460**	
Met (M)	12	1							6
Phe (F)		1					2		41
Pro (P)	45	2	**3**						
Ser (S)	231	803	**1868**		220		1		
Thr (T)	28	**3211**	5	**528**	12		1		
Trp (W)	14								
Tyr (Y)									
Val (V)				1	3		**444**		1
Total	4737	4253	3556	531	512	469	465	466	466

818
819

820 All HCV genotype 2 E2 amino acid sequences in the ViPR database were aligned and the
821 number of sequences containing each residue at the sites of our adaptive mutations was
822 determined.

823 **Table 4: Summary of properties of the growth adaptive E2 variants**

Virus	H77 Residue	RNA: $TCID_{50}$*	H77.39*	HC84.26*	CD81LEL*	anti-CD81**	anti-CLDN1**	anti-SRBI***	$SRBI^{KO}$***
Q412R	Q412	1.7	19	8.4	2.1	2.2	2.0	82%	58%
T416R	T416	2.3	63	6.5	5.5	2.8	1.4	72%	57%
S449P	S449	2.0	46	11	1.5	0.91	1.9	100%	59%
T563V	T561	3.3	26	9.7	6.2	1.4	1.3	55%	55%
A579R	(N577)	3.8	2.8	1.0	1.1	2.6	1.5	34%	33%
L619T	L615	2.6	28	6.0	10	3.3	1.7	100%	61%
V626S	I622	1.5	4.9	2.6	1.6	2.6	2.7	57%	44%
K632T	K628	1.2	1.2	1.7	0.44	2.1	4.4	36%	44%
L644I	L640	1.3	3.8	4.5	1.7	1.2	2.7	53%	58%

824 *Fold reduction
825 **Fold increase
826 ***Resistant fraction
827 A summary of the properties of the mutants identified in this study. Fold decrease relative to
828 parent is listed for RNA:$TCID_{50}$. The fold change in EC_{50} (increase or decrease) is listed for all
829 dose-response inhibition assays. For the SR-BI antibody dose response or infection of $SR\text{-}BI^{KO}$
830 cells, the fraction of virus resistant to SR-BI blockade or deletion is listed.

831

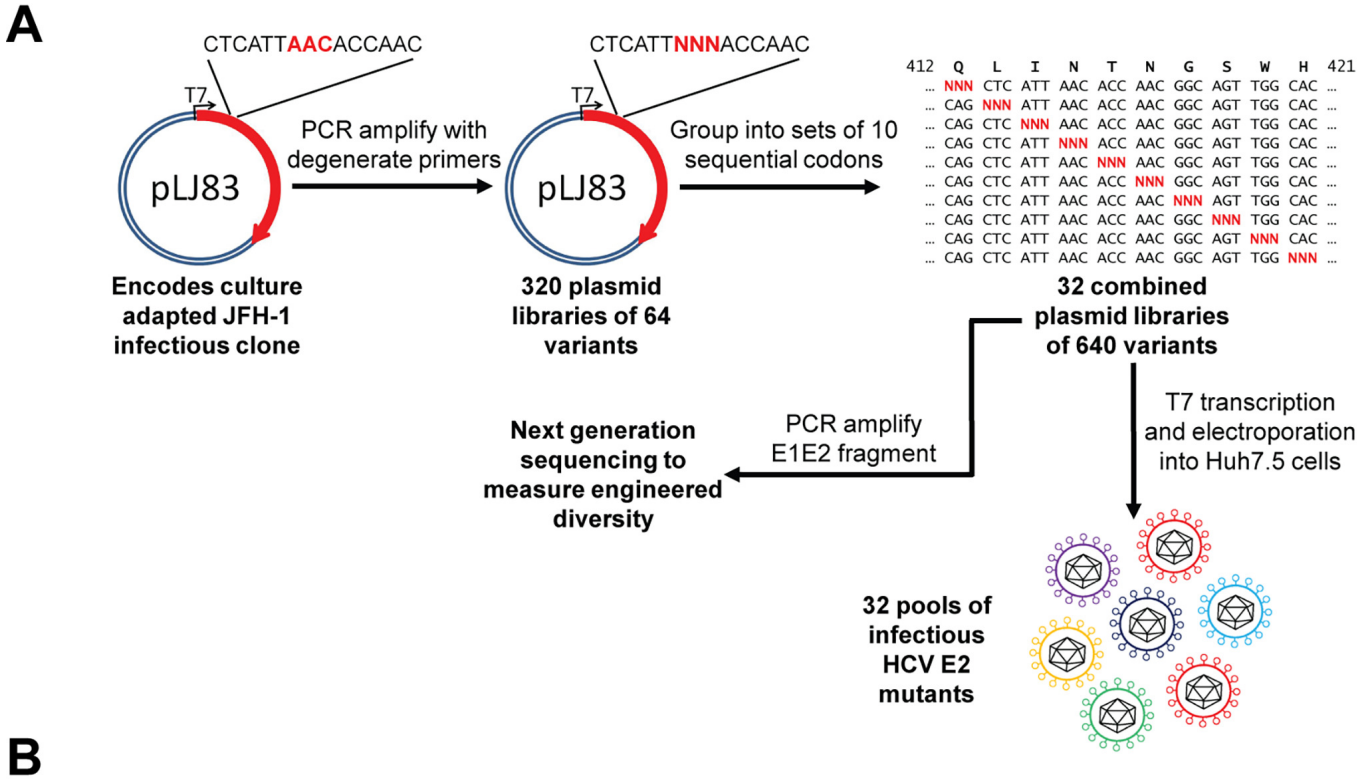

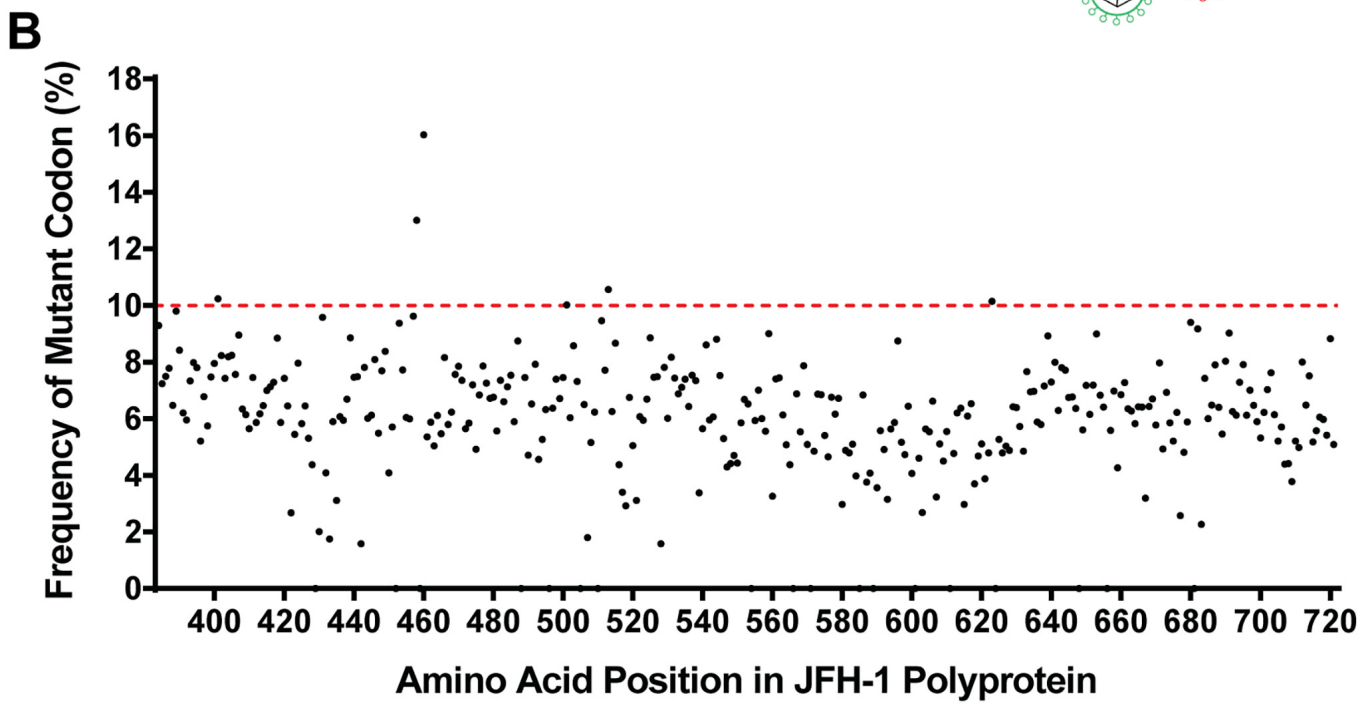

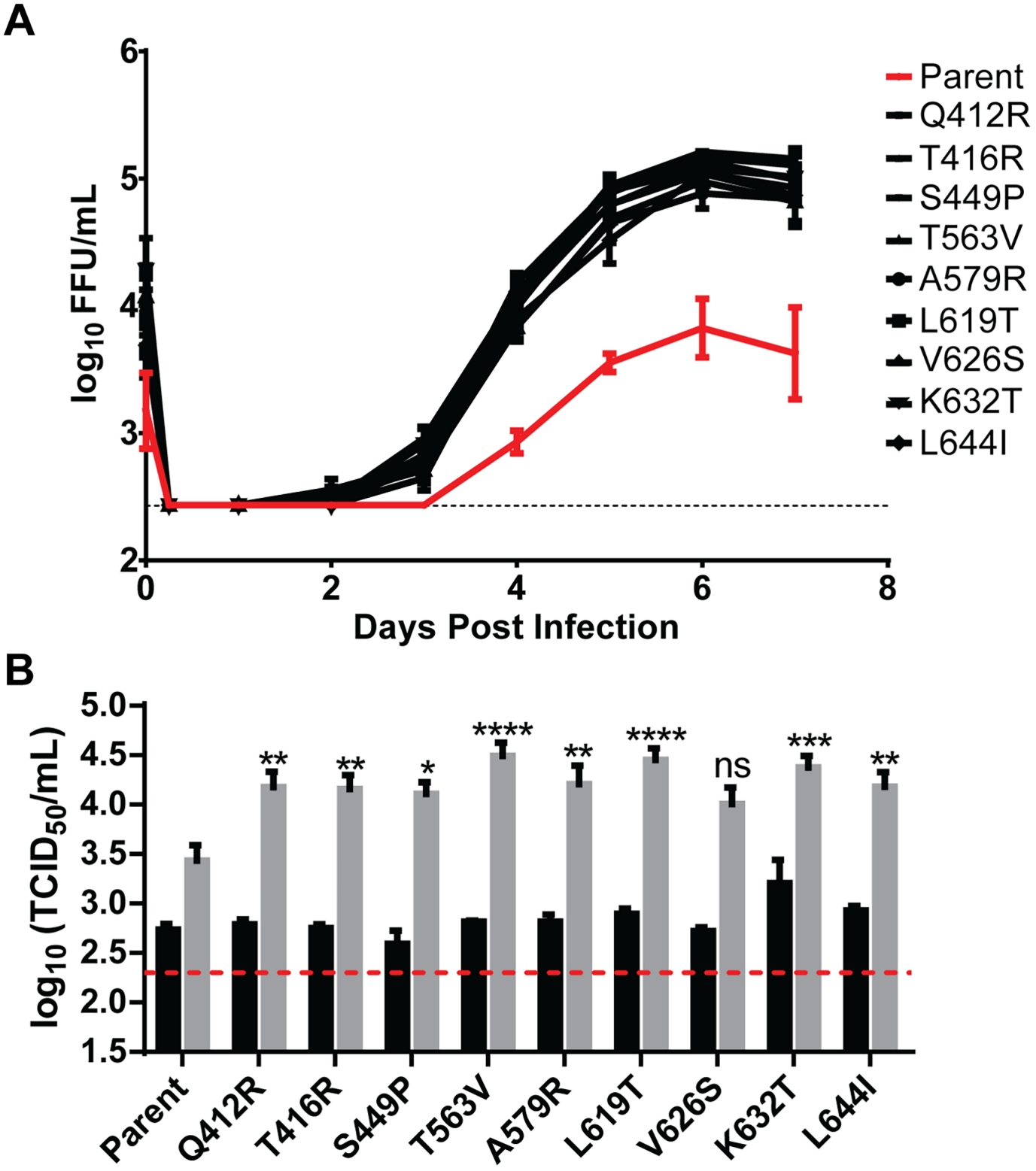

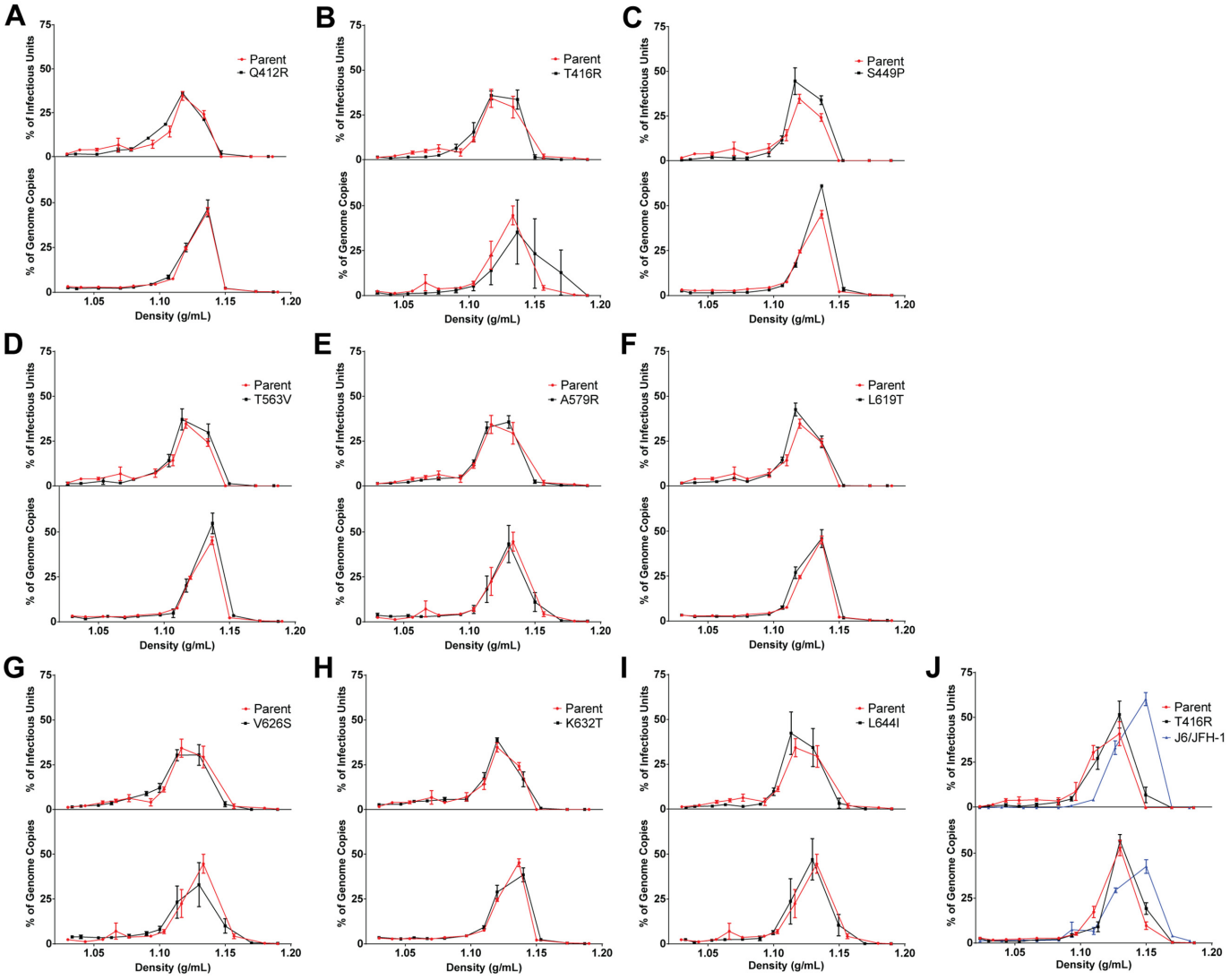

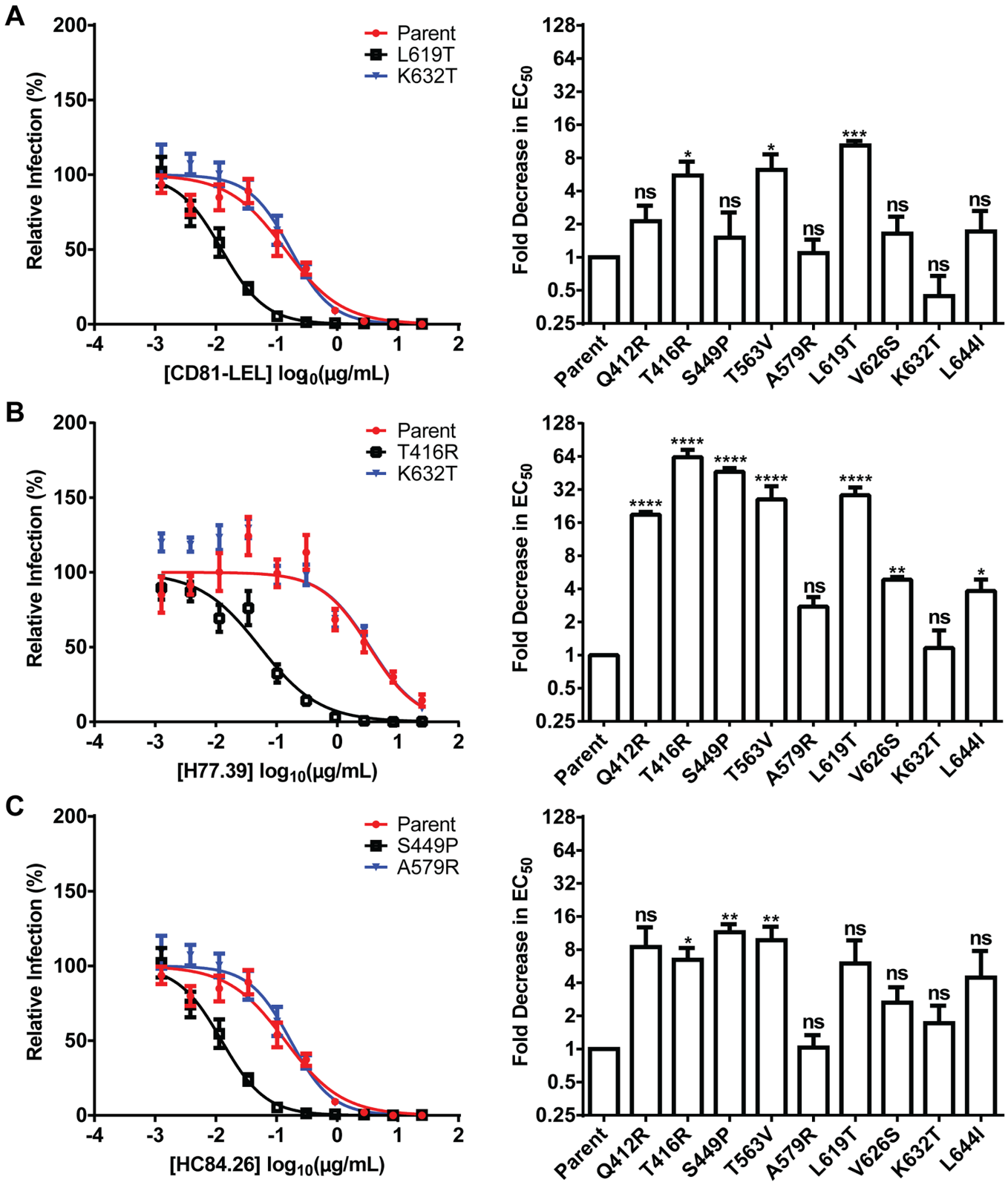

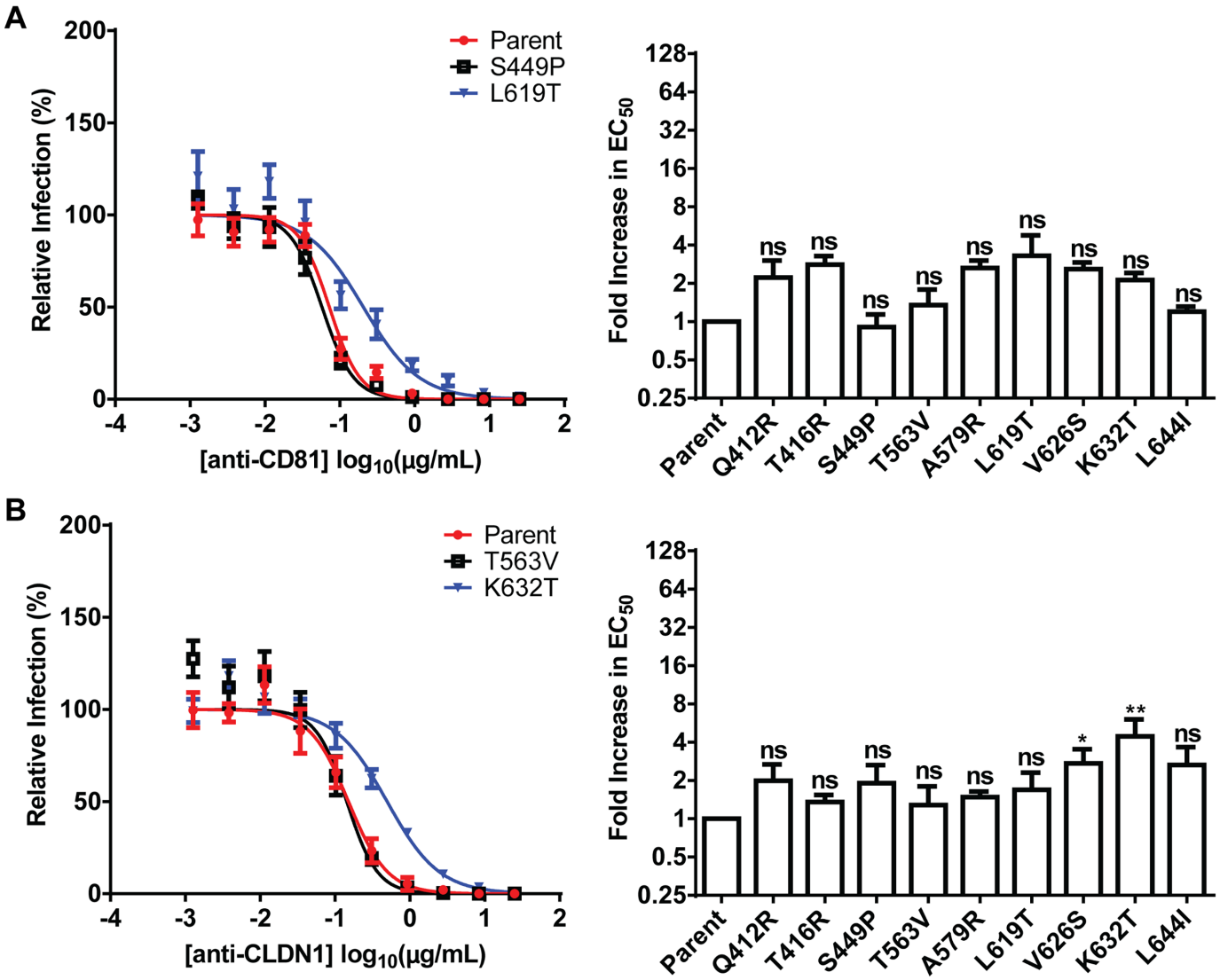

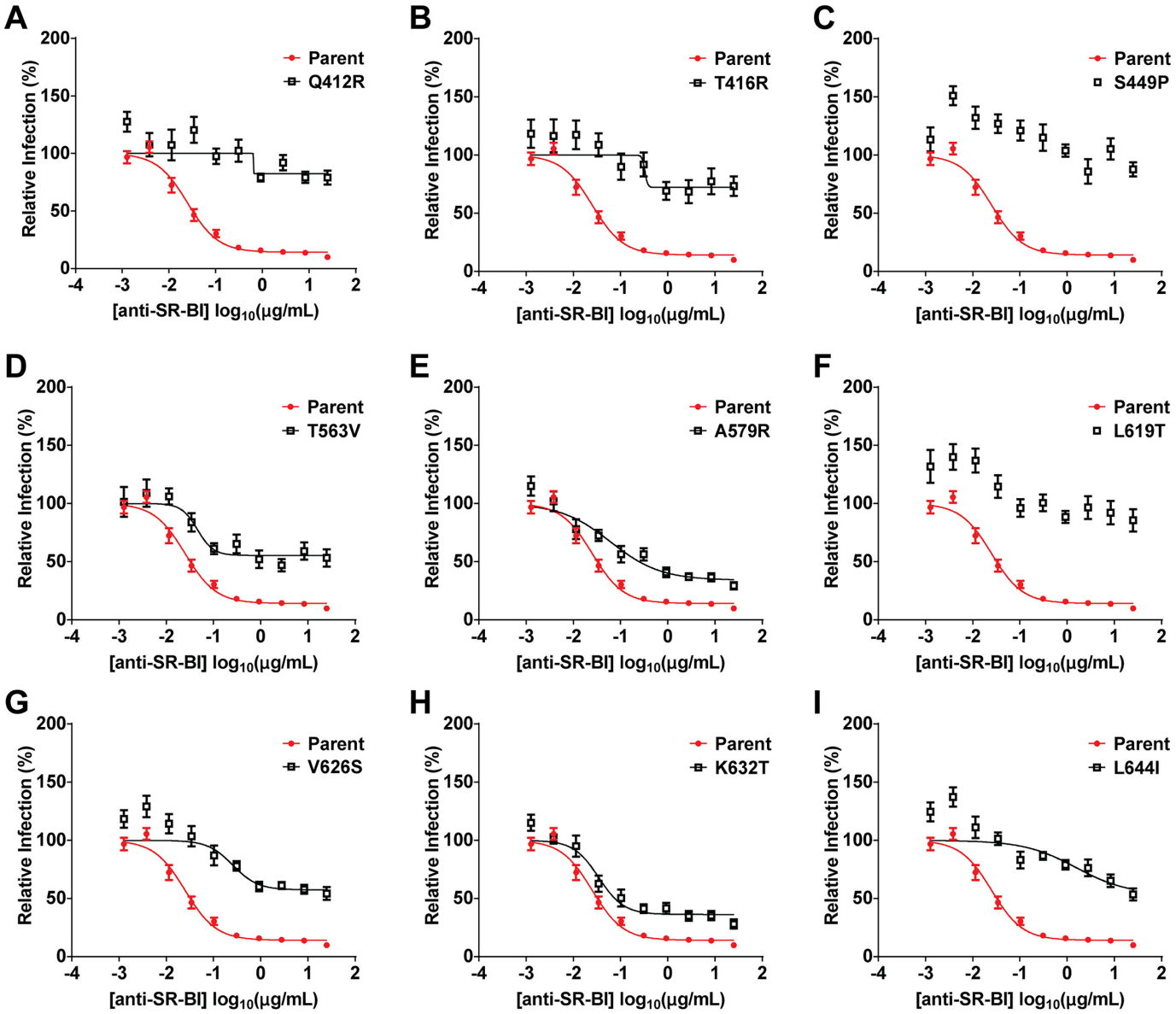

Journal of Virology